

# Ant Colony Optimization based MRI Brain Image Despeckling

Sanjeev Acharya

Computer Science & Engg., Mansarovar Institute of Technology and Science Bhopal, India  
Email: acharya.sanjeev@ymail.com

**Abstract** - This paper determines the Magnetic resonance image despeckling issues with ACO (Ant Colony Optimization) in wavelet domain. This paper proposes the approach for image noise reduction with comparison of generalized unsupervised masking used median filter. This method consists three approaches. Firstly, it masks the image, secondly applies ant searching then and finally denoise it. Proposed method is automatically adapted to observing image data in lieu of imposed assumptions of image data. Experimental results included for the comparisons of this approach.

**Keywords**-MRI, ACO, Median Filter, Masking

## I. INTRODUCTION

MRI machines make use of the fact that body tissue contains lots of water, and hence protons ( $^1\text{H}$  nuclei), which will be aligned in a large magnetic field. Each water molecule has two hydrogen nuclei or protons. When a person is inside the powerful magnetic field of the scanner, the average magnetic moment of many protons becomes aligned with the direction of the field. A radio frequency current is briefly turned on, producing a varying electromagnetic field. This electromagnetic field has just the right frequency, known as the resonance frequency, to be absorbed and flip the spin of the protons in the magnetic field. After the electromagnetic field is turned off, the spins of the protons return to thermodynamic equilibrium and the bulk magnetization becomes realigned with the static magnetic field. During this relaxation, a radio frequency signal (electromagnetic radiation in the RF range) is generated, which can be measured with receiver coils. Information about the origin of the signal in 3D space can be learned by applying additional magnetic fields during the scan. These additional magnetic fields can be used to generate detectable signals only from specific locations in the body (spatial excitation) and/or to make magnetization

at different spatial locations precess at different frequencies, which enables k-space encoding of spatial information. The 3D images obtained in MRI can be rotated along arbitrary orientations and manipulated by the doctor to be better able to detect tiny changes of structures within the body. [5] These fields, generated by passing electric currents through gradient coils, make the magnetic field strength vary depending on the position within the magnet. Because this makes the frequency of the released radio signal also dependent on its origin in a predictable manner, the distribution of protons in the body can be mathematically recovered from the signal, typically by the use of inverse Fourier transform. Removing speckle noise plays a key role in medical image processing (e.g., medical ultrasonography), since the speckle noise significantly degrades the image quality and complicates diagnostic decisions for discriminating fine details in images [6,7]. A noisy image in spatial domain can be formulated as original image with the additive or the multiplicative noise.

## II. LITERATURE SURVEY

According to [6], three-dimensional denoising of magnetic resonance images that exploit the sparseness and self-similarity properties of the images. Are based on a three-dimensional moving-window discrete cosine transform hard thresholding and a three-dimensional rotationally invariant version of the well-known nonlocal means filter. Both methods run in less than a minute, making them usable in most clinical and research settings [6]. There are many speckle reduction filters available, some give better visual interpretations while others have good noise reduction or smoothing capabilities. Some of the best known speckle reduction filters are Median, Lee, Kuan, standard Frost, Enhanced Frost, Weiner, Gamma MAP and SRAD filters.

Some of these filters have unique speckle reduction approach that performs Spatial filtering in a square-moving window known as kernel. The filtering is based on the statistical relationship between the center pixel and its surrounding pixels. The typical size of filter window can range from 3-by-3 to 33-by-33, but the size of window must be odd. If the size of the filter window is too large, important details will be lost due to over smoothing. On the other hand, if the size of the window is too small, speckle reduction may not yield good results. Generally a 3-by-3 or 7-by-7 window is used giving good results [3]. The Median Filter [4] computes the median of all the pixels within a local window and replaces the center pixel with this median value. Median filtering is a non-linear filtering technique. This method is effective in cases when the noise pattern consists of strong, spike like components and the characteristics to be preserved are edges. The main disadvantage of the median filter is the extra computation time needed to sort the intensity value of each set. The Wiener Filter [5], also known as Least Mean Square filter, is given by the following expression:  $H(u, v)$  is the degradation function and  $H(u, v)^*$  is its conjugate complex.  $G(u, v)$  is the degraded image. Functions  $S_f(u, v)$  and  $S_n(u, v)$  are power spectra of original image and the noise. Wiener Filter assumes noise and power spectra of object a priori.

$$f(u, v) = [H(u, v)^* / H(u, v) + \frac{S_n(u, v)}{S_f(u, v)}] G(u, v) \quad --(1)$$

Lee Filter[6] is based on multiplicative speckle model and it can use local statistics to effectively preserve edges.

This filter is based on the approach that if the variance over an area is low or constant, then smoothing will not be performed, otherwise smoothing will be performed if variance is high (near edges).

$$Img(\odot, j) = Im + W * (Cp - Im) \quad --(2)$$

Where  $Img$  is the pixel Value at indices  $\odot, j$  after filtering,  $Im$  is mean intensity of the filter window,  $Cp$  is the center pixel and  $W$  is a filter window given by:

$$W = \sigma^2 / (\sigma^2 + \rho^2) \quad --(3)$$

where  $\sigma^2$  is the variance of the pixel values within the filter window and is calculated as:

$$\sigma^2 = \left[ \frac{1}{N \sum_{j=0}^{N-1} X_j^2} \right] \quad --(4)$$

Here,  $N$  is the size of the filter window and  $X_j$  is the pixel value within the filter window at indices  $j$ . The parameter  $\rho$  is the additive noise variance of the image. When light is passed through both negative and in-register positive (in an enlarger for example), the positive partially cancels some of the information in the negative. Because the positive has been intentionally blurred, only the low frequency (blurred) information is cancelled. In addition, the mask effectively reduces the dynamic range of the original negative. Thus, if the resulting enlarged image is recorded on contrasty photographic paper, the partial cancellation emphasizes the high frequency (fine detail) information in the original, without loss of highlight or shadow detail. The resulting print appears sharper than one made without the unsharp mask: its acutance is increased. Unsharp masking may also be used with a large radius and a small amount (such as 30–100 pixel radius and 5–20% amount which yields increased local contrast, a technique termed local contrast enhancement [5]. USM can increase either sharpness or (local) contrast because these are both forms of increasing differences between values, increasing slope – sharpness referring to very small-scale (high frequency) differences, and contrast referring to larger scale (low frequency) differences. More powerful techniques for improving tonality are referred to as tone mapping.

A noisy image in spatial domain can be mathematically formulated as

$$g_i = f_i \epsilon_i \quad --(5)$$

where  $\odot$  represents the pixel index,  $g_i$  is the noisy pixel,  $f_i$  is the noise-free pixel and  $\epsilon_i$  represents the speckle noise [7]. The multiplicative noise in (5) can be converted to an additive one by applying

$$g_i^l = f_i^l + \epsilon_i^l \quad --(6)$$

$g_i^l$ ,  $f_i^l$  and  $\epsilon_i^l$  are log-transformed versions of  $g_i$ ,  $f_i$  and  $\epsilon_i$ , respectively. It has been justified in the literature that the distribution of the log transformed speckle is close to a Gaussian distribution [5,6]. Furthermore, since the discrete wavelet transform is a linear operation, the wavelet coefficients of the logtransformed image corrupted by the speckle noise can be expressed the log-transformation on both sides of (5) to arrive at

$$y_i = x_i + n_i \quad --(7)$$

Where  $y_i$ ,  $x_i$  and  $n_i$  represent wavelet coefficients of  $g_i^l$ ,  $f_i^l$  and  $\epsilon_i^l$  respectively. The mathematical relation between image's intensity information and their wavelet coefficients can be found in [8,9]. Based on the above formulations, the goal of image denoising is to recover each noise-free coefficient  $x_i$  based on its noisy counterpart  $y_i$ .

### III. IMAGE ACQUISITION

The MRI brain image consists of film artifacts or label on the MRI such as patient name, age and marks. Film artifacts that are removed. The intensity value of the pixels are analyzed and the threshold value of the film artifacts are found. The threshold value, greater than that of the threshold value is removed from MRI. The high intensity values of film artifacts are removed from MRI brain image. The following figures explain the process of preprocessing stage. A sample of 80 T1 weighted images are taken and used for enhancement purpose. T1- weighted images shows water darker and the fat brighter. An image of a patient obtained by MRI scan is displayed as an array of Pixels (a Two Dimensional unit based on the matrix size and the field of view) are stored. Images are three types (a) Binary Images (b) Gray Scale Image (c) Color Image. In this paper, we consider grayscale or Intensity Images to display an image with default size of 256 x 256[8]. The following figure (3.1) displays a MRI Brain Image. A grayscale Image can be specified by giving a large matrix whose entries are

numbers between 0 and 255, with 0 to black and 255 to white.

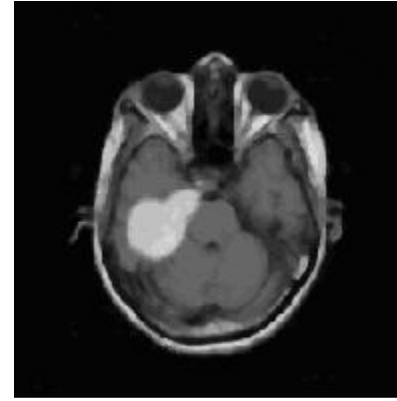


Figure 3.1

### IV. PROPOSED METHODOLOGY

Ant colony optimization (ACO) is currently a popular algorithm [9]. The classical application is to routing in telecommunication networks. ACO model is natural ant inspired for the problem solving, while the ant searches food from their nest to, where they found food deposits, the ants deposit trail of chemical material pheromone which attracts another ant, quickly ant mobilised to the food direction and this path become the sought chance for food accumulation from destination to nest. A shorter path from source to destination has been discovered. But, the pheromones evaporates, so other ants then follow quickly which suites them. In this study ants first relate neighbourhoods to find solution, they select an image with  $N \times N$  size then we add noise in it using equation (7) which is additive noise.

$W_{N_n(s)}$  neighbourhood calculation according to the  $(N_n + 1) \times (N_n + 1)$  size neighbourhood around image  $s$  simply adding noise from equation (8)

$$G = (rand(n_i) + t rand(x)) \times S \quad --(8)$$

And applied on a two-level decomposition using a Daubechies's wavelet with eight vanishing moments. Then, the distributions of the second-level detail subbands are fitted with the above-mentioned models, which are further compared with the histogram of the wavelet coefficients in

the sense of the above-mentioned two statistical metrics. We also apply here cumulative density function CDF. The importance of the original Ant System (AS) [11, 12, 13] resides mainly in being the prototype of a number of ant algorithms which collectively implement the ACO paradigm. AS already follows the outline presented in the previous subsection, specifying its elements as follows. The move probability distribution defines probabilities the functioning of an ACO algorithm can be summarized as a set of computational concurrent and asynchronous agents (a colony of ants) moves through states of the problem corresponding to partial solutions of the problem to solve. They move by applying a stochastic local decision policy based on two parameters, called trails and attractiveness. By moving, each ant incrementally constructs a solution to the problem. When an ant completes a solution, or during the construction phase, the ant evaluates the solution and modifies the trail value on the components used in its solution. This pheromone information will direct the search of the future ants. Furthermore, an ACO algorithm includes two more mechanisms: trail evaporation and, optionally, daemon actions. Trail evaporation decreases all trail values over time, in order to avoid unlimited accumulation of trails over some component. Daemon actions can be used to implement centralized actions which cannot be performed by single ants, such as the invocation of a local optimization process. Probability  $P_{t\psi^k}$ , of moving from state  $t$  to state  $\psi$  in  $k$  steps.

Where, attractiveness  $\eta_{t\psi}$  of the move which is a priori of movement and  $\tau_{t\psi}$  trail level of movement.

The probability is defined as follows,

$$P_{t\psi^k} = \begin{cases} \frac{\tau_{t\psi}^\alpha + \eta_{t\psi}^\beta}{\sum_{(t\zeta \in \text{tabu}^k)} (\tau_{t\zeta}^\alpha + \eta_{t\zeta}^\beta)} & \text{--(9)} \\ \text{if } (t\psi) \notin \text{tabu}^k & \\ \text{otherwise} & \end{cases}$$

otherwise

Where  $\alpha$  and  $\beta$  are user defined parameters. In equation (9)  $\text{tabu}^k$  is the tabulation list of ant  $k$ , while parameters  $\alpha$  and  $\beta$  are trail and attractiveness.

After each iteration determine from the number of pixels is  $t$  in algorithm, when all ants completed solutions, trail values are updated by means of pheromone updates by following formula,

$$\tau_{t\psi}(\tau) = (\tau - 1)\rho\tau_{t\psi} + \Delta\tau_{t\psi} \quad \text{--(10)}$$

Where  $\rho$ ,  $0 \leq \rho \leq 1$ , evaporation coefficient  $\Delta\tau_{t\psi}$  sum of contribution of all ants.

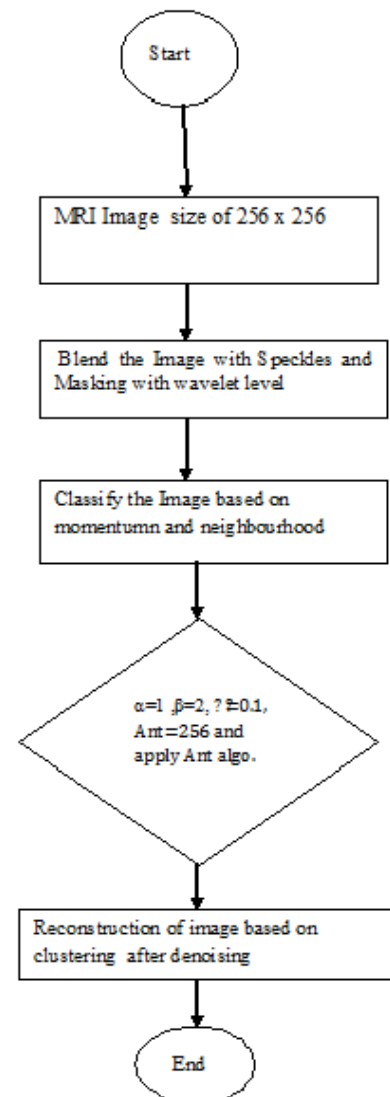


Figure 4.1 Flow Diagram

1. Compute a (linear) lower bound LB and upper bound UB for image.

Initialize variables with the values

2. For  $k=1, m$  ( $m$ = number of ants) do
  - repeat
    - 2.1 Compute values of equation(9)
    - 2.2 Choose in probability the state to move into grid
    - 2.3 Append the chosen move to the  $k$ -thant's position in list until ant  $k$  has completed its solution
    - 2.4 Carry the solution to its local optimum by (min,max) Row and (min,max)col Pixels End for
  3. For each ant move ( $\psi$ ), compute  $\Delta\tau\psi$  and update trails by means of equation(10)
  4. If not(end test) goto step 2.

## V. EXPERIMENTAL RESULT ANALYSIS\

We have Taken Three test Images as shown in figure 5.1 and check the performanace on exixsting and Proposed methodology.

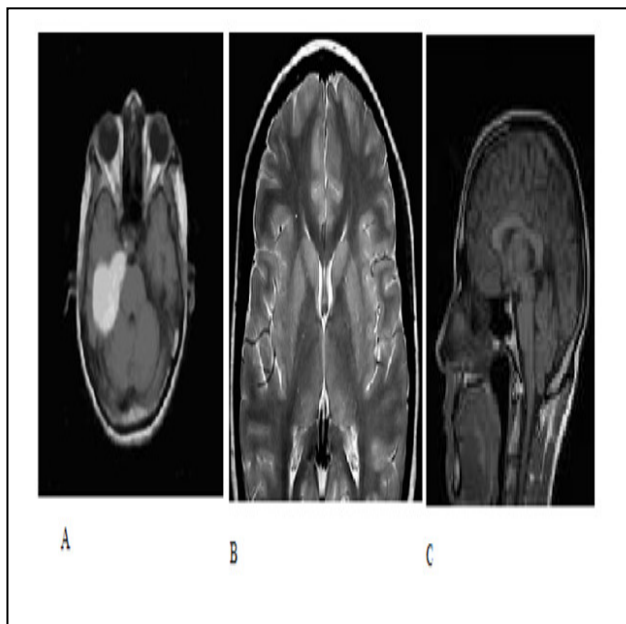


Figure 5.1

With various values of noise in the given Table 5.1

Image	Noise %	FcnFrost Filter Method(dB)	Proposed Method (dB)
A	10	18.95	34.33
	40	16.52	23.43
	60	10.56	17.66
B	10	23.83	41.49
	40	21.57	31.10
	60	20.88	27.89
C	10	20.33	36.11
	40	17.43	27.69
	60	14.25	21.74

Table 5.1

Figure 5.2 Depicts the graphical comparison of Proposed Method with existing method.

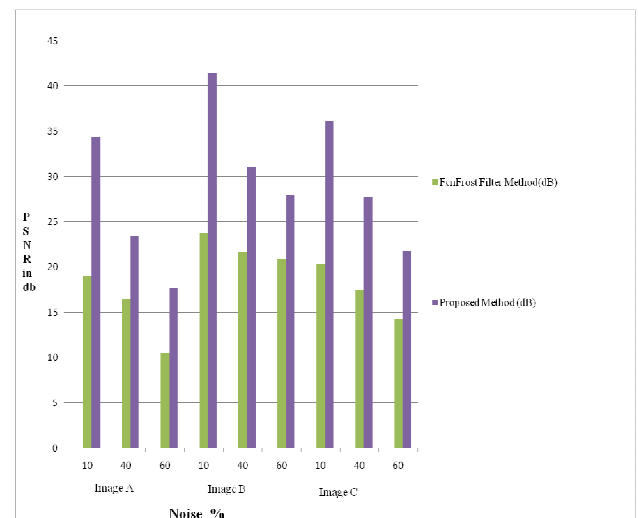


Figure 5.2

## VI. CONCLUSION AND REMARKS

Image despeckling involves a vast problem set which includes different problems faced in image processing itself. An ant colony optimization based despeckling approach has been proposed by incorporating a combinatorial problem. Paper makes a true work to cover all possible combinations

and worked done on it explained through the reference. An attempt is made to do a study and reading all the listed references. Future work for this survey would include, making a more detailed comparative study on the pixelwise analysis. Including more researches as they appear to be related to the topic with best of our knowledge.

## REFERNCES

- [1] Latha Parthiban, R. Subramanian, "Speckle Noise Removal Using Contoulets " IEEE, Conference on Information and Automation, p.p . 250-253, 2006.
- [2] S.G. change, B. Yu, and M. vetterli, "Adoptive wavelet thresholding for image denoising and compression", *IEEE Trans.Image Process*, vol.9, no. 9, pp. 1532, Sep. 2000
- [3] R. F. Wagner, S. W. Smith, J. M. Sandrik and H.Lopez, "Statistics of Speckle in Ultrasound BBXcans," *IEEE Trans. Sonics Ultrasonics* 30, 1983, 156–163.
- [4] Khaled Z. AbdElmoniem, Yasser M. Kadah and AbouBakr M. Youssef, "Real Time Adaptive Ultrasound Speckle Reduction and Coherence Enhancement", 0780329772000 IEEE, pp. 172-175.
- [5] G. Ramponi, N. Strobel, S. K. Mitra and T. Yu, "Nonlinear unsharp masking methods for image contrast enhancement", *Journal of Electronic Imaging*, Vol. 5(3), July 1996, pp. 353-366.
- [6] J. Lee, L. Jurkevich, P. Dewaele, P. Wambacq, A. Oosterlinck, Speckle filtering of synthetic aperture radar images: a review, *Remote Sens. Rev.* 8 (1994) 313–340.
- [7] R. Touzi, A review of speckle filtering in the context of estimation theory, *IEEE Trans. Geosci. Remote Sens.* 40 (2002) 2392–2404.
- [8] George E.B.,Karnan M., "MRI Brain Image Enhancement Using Filtering Techniques", *International Journal of Computer Science & Engineering Technology (IJCSET)*, 2012.
- [9] M. Dorigo, V. Maniezzo, and A. Colomi, "The ant system: Optimizatio n by a colony of cooperating agents," *IEEE Trans. Syst., Man, Cybern. B, Cybern.*, vol. 26, no. 1, pp. 29–41, Feb. 1996.
- [10] A. Colomi, M. Dorigo, V. Maniezzo (1991) Distributed optimization by ant colonies, In *Proceedings of ECAL'91 European Conference on Artificial Life*, Elsevier Publishing, Amsterdam, The Netherlands, pp 134-142.
- [11] M. Dorigo (1992) "Optimization, learning and natural algorithms", Ph.D. Thesis, Politecnico di Milano, Milano
- [12] M. Dorigo, V. Maniezzo, A. Colomi (1991) The ant system: an autocatalytic optimizing process, Technical Report TR91-016, Politecnico di Milano.
- [13] D. Donoho, I. Johnstone, Adapting to unknown smoothness via wavelet shrinkage, *J. Am. Statist. Assoc.* 90 (1995) 1200–1224.
- [14] J. Tian, W. Yu, L. Ma, AntShrink: Ant colony optimization for image shrinkage, *Pattern Recogn. Lett.* 31 (2010) 1751–1758.
- [15] L. Wasserman, *All of Statistics*, Springer, 2004.
- [16] A. Pizurica, R. Pizurica, W. Philips, I. Lemahieu, M. Acheroy, A versatile wavelet domain noise filtration technique for medical imaging, *IEEE Trans. Med. Imaging* 22 (2003) 323–331.
- [17] L. Kaur, S. Gupta, R. Chauhan, Image denoising using wavelet thresholding, in: *Proc. Int. Conf. on Computer Vision, Graphics and Image Processing*, Ahmadabad, India, 2002, pp. 1–6.
- [18] F. Luisier, T. Blu, M. Unser, A new SURE approach to image denoising: interscale orthonormal wavelet thresholding, *IEEE Trans. Image Process.* 16 (2007) 593–606.
- [19] D. Zhou, W. Cheng, Image denoising with an optimal threshold and neighbouring window, *Pattern Recogn. Lett.* 19 (2008) 1694–1697.